ELSEVIER

Journal of Molecular Catalysis B: Enzymatic 15 (2001) 29–43

JOURNAL OF MOLECULAR CATALYSIS B: ENZYMATIC

www.elsevier.com/locate/molcatb

Studies on the reaction mechanism of RNAse T1 with quantum chemical reactivity indexes

Piet Demeester

Av. G. Demey 112/5 1160, Brussels, Belgium

Received 25 August 2000; accepted 22 December 2000

Abstract

The reaction mechanism of RNAse T1 has been investigated with natural bond orbital (NBO) methods, the Mulliken population analysis and the condensed Fukui function. The natural condensed Fukui function is introduced for use in chemistry. The computational results are brought in connection with experimental findings. It is shown how significant delocalisation of the orbitals occurs during catalysis and that an enzyme can change the weight of a resonance structure.

Keywords: NBO analysis; Enzyme catalysis; Fukui function; RNAse T1; Charge transfer interaction

1. Introduction

In this paper, it is shown how enzyme catalysis can be treated in terms of Lewis acid/base interactions and how reactivity indexes that relate to the interaction energy, assist in the interpretation of Lewis structures. With the help of natural bond orbital analysis it is shown that van der Waals bonds begin to look like covalent bonds during enzyme catalysis and that the enzyme can change the weight of a resonance structure to fit its needs.

1.1. Overview of biochemical research

RNAse T1 [1] is a guanine specific ribonuclease of Aspergillus Oryzae. It cleaves the P-O5′ ester bond of GpN sequences of single stranded RNA. A stable 2′, 3′ cyclophosphate intermediate is then formed and can be hydrolysed to form 3′ guanylic acid. Eckstein et al. [2] concluded that the reaction proceeds through inversion of configuration. Osterman and Waltz [3] showed that the activity of the wild type enzyme depends on two protonated functional groups and two deprotonated functional groups. Steyaert et al. [4] compared the pH profile of k_{cat}/K_m and k_{cat} of His40Lys and Glu58Ala mutants with the wild type enzyme. They concluded that the catalysis in the wild type enzyme depends on the protonated form of His40 and that His40 will become deprotonated in the Glu58Ala mutant and take over the role of Glu58 as the acid catalyst.

The residues Asn36 and Asn98 enhance the catalytic activity of the enzyme through an interaction with the leaving nucleotide of dinucleotide substrates, and Tyr38 is a residue that directly contributes to catalysis [5].

Doumen et al. [6] attributed a catalytic function to Phe100. They found that its catalytic function does not proceed via a subsite interaction. There was no functional interaction between Phe100 and His92 during catalysis but a significant functional interaction is observed upon substrate binding. The mutation of Phe100 causes some structural change in the active

E-mail address: piet.demeester@skynet.be (P. Demeester).

1381-1177/01/$ – see front matter
PII: S1381-1177(01)00002-9

site due to the large cavity left after removing this group.

Loverix et al. [7] showed that RNAse T1 catalyses the formation of 2′, 3′GMP from 3′GMP because there was a time dependent wash-in of solvent O^{18} in 3′GMP.

2. Theory

2.1. Theoretical treatment of the generalised Lewis acid/base reactions

I will investigate the interaction between an enzyme and a substrate in terms of the properties of the chemical bonds that are formed or can be formed. The Lewis acid/base concept is deeply rooted into theoretical science and ideally used for this purpose. Pearson [8] contributed considerably to the understanding of Lewis acid/base interactions with his formulation of the hard and soft acids and bases principle (the HSAB principle): "Hard likes Hard and Soft likes Soft". The HSAB principle has found a sound theoretical basis and proof in the density functional theory, where Chattaraj, Lee et al. [9] have shown that the energetic stabilisation during a Lewis acid/base interaction is a consequence of two opposing factors, the electronegativity equalisation principle [10] and the maximum hardness principle [11]. The electronic chemical potential [1], which naturally arises from the density functional theory [12], has been identified with the negative of the electronegativity [13]. And the electronegativity can be defined by Mulliken's formula ($(I + A)/2$), i.e. half of the sum of the ionisation energy and the electron affinity of the chemical species under investigation. The maximum hardness principle has been proven independently by Parr and Chattaraj by making use of the fluctuation-dissipation theorem of statistical mechanics [11].

Several important reactivity indexes that can be used to characterise Lewis acid and base interactions, have been derived from the basic equation for the change of one ground state to another from the density functional theory [14]

$$\mathrm{d}E = \mu\,\mathrm{d}N + \int \rho(r)v(r)\,\mathrm{d}r \tag{1}$$

itself a product of the famous theorem of Hohenberg and Kohn [15].

A Taylor series expansion to second order of this equation can be obtained (2):

$$\begin{aligned}\Delta E = {} & \left(\frac{\partial E}{\partial N}\right)_{v(r)} \Delta N + \int \left(\frac{\partial E}{\partial v(r)}\right)_{N} \Delta v(r)\,\mathrm{d}r \\ & + \int \left(\frac{\partial^2 E}{\partial N \partial v(r)}\right) \Delta N \Delta v(r)\,\mathrm{d}r \\ & + \frac{1}{2}\left(\frac{\partial^2 E}{\partial^2 N}\right)_{v(r)} \Delta N^2 \\ & + \frac{1}{2}\int \left(\frac{\partial^2 E}{\partial v(r)\partial v(r')}\right)_{N} \Delta v(r)\Delta v(r')\,\mathrm{d}r\,\mathrm{d}r'\end{aligned} \tag{2}$$

we can attribute a chemical relevant meaning to several of the terms.

The electronic chemical potential (first term), being the negative of the electronegativity is defined as

$$\mu = \left(\frac{\partial E}{\partial N}\right)_{v(r)} \tag{3}$$

where E is the energy, N the number of electrons and $v(r)$ the electrostatic potential that the electrons experience due to the nuclei, r and r' are independent spatial co-ordinates. All quantities considered here and in the sequel are given in atomic units.The chemical hardness (fourth term) is defined as

$$\eta = \frac{1}{2}\left(\frac{\partial^2 \mu}{\partial^2 N}\right)_{v(r)} \tag{4}$$

The density functional theory definition of the electron density is given by (second term).

$$\rho(r) = \left(\frac{\partial E}{\partial v(r)}\right)_{N} \tag{5}$$

here the functional derivative was taken.

Making use of the former statement (5) we can write for the third term

$$f(r) = \left(\frac{\partial \rho(r)}{\partial N}\right)_{v(r)} \tag{6}$$

[1] This term may not be confused with the chemical potential from thermodynamics, it is related to this quantity because in the density functional theory the system under investigation is the equilibrium state of a grand canonical ensemble at 0 K. The chemical potential from the grand canonical ensemble is related to the thermodynamic chemical potential.

Here $f(r)$ is called the Fukui function (i.e. the frontier electron density) [16]. Parr and Berkowitz [17] have derived an expression for the last term of Eq. (2). Li and Evans [18], who have treated this term in detail, obtained an expression in terms of the quantities here defined.

While Eq. (2) gives the change of energy of one system under the influence of an interaction we can write down an equation for the change in energy when two systems (k and l) interact.

$$\Delta E_{\text{total}} = \Delta E_k + \Delta E_l \tag{7}$$

$$\Delta E_{\text{total}} = (\mu_k - \mu_l)\Delta N + (\eta_k + \eta_l)\Delta N^2 \tag{8}$$

$$+ \int \{\rho_k(r)\Delta v_k(r) + \rho_l(r)\Delta v_l(r)\}\,\mathrm{d}r + \Delta N \int \{f_k(r)\Delta v_k(r) - f_l(r)\Delta v_l(r)\}\,\mathrm{d}r \tag{9}$$

$$+ \iint \left[\frac{\partial \rho_k(r)}{\partial v_k(r')}\right]_{Nk} \Delta v_k(r)\Delta v_k(r')\,\mathrm{d}r\,\mathrm{d}r' + \iint \left[\frac{\partial \rho_l(r)}{\partial v_l(r')}\right]_{Nl} \Delta v_l(r)\Delta v_l(r')\,\mathrm{d}r\,\mathrm{d}r' \tag{10}$$

This expression shows how quantities Eqs. (3)–(6) are related to the change in energy during an interaction. Making use of the finite difference approximation we can write:

$$\mu = \frac{I + A}{2} \quad \text{and} \quad \eta = \frac{I - A}{2}$$

$$f^+(r) = \rho_{N+1}(r) - \rho_N(r),$$

$$f^-(r) = \rho_N(r) - \rho_{N-1}(r),$$

$$f^0(r) = \tfrac{1}{2}[\rho_{\text{HOMO}}(r) + \rho_{\text{LUMO}}(r)]$$

where I and A are the ionisation energy and the electronaffinity, respectively, and I have taken the right and left derivative for the Fukui function.

The quantities from Eq. (8) are global quantities of the system and are essentially the electronegativity and half the band gap between the highest occupied molecular orbital and the lowest unoccupied molecular orbital. The first term of Eq. (9) is the Coulomb interaction between two systems and the second represents the energy stabilisation due to the orbital interactions between the two systems. The last term is always negative due to the linear response function [19]. The term η is related to the hardness of Pearson [20] and it can be shown that the hardness acts against electron transfer and is inversely proportional to the energy lowering during charge transfer [21]. The expressions in Eq. (9) are local quantities (i.e. their value is dependent on the spatial co-ordinate r) and can thus be used as selectivity indexes.

It is important to realise that all of these quantities have obtained a meaning in chemistry independent of their derivation from the basic equations of the density functional theory.

By making use of the generalised polyelectronic perturbation theory Klopman [22] was able to derive an expression for the interaction between an electron donor and an electron acceptor. He then identified charge controlled and frontier-controlled interactions.

Fujimoto and Fukui [23] showed that it is possible to approximate the common wave function of two interacting systems by a linear combination of the wave functions of the adiabatic interaction (both systems in the ground state), the charge transfer reaction (one electron transferred from one system to the other) and the polarisation interaction (one electron excited). They then obtained an expression that subdivides the interaction energy into four terms, Coulomb interaction, exchange interaction (which arises due to Pauli's exclusion principle and the subsequent use of Slater determinants to approximate the wave function), delocalisation and polarisation interaction.

It was Fukui who first proposed the use of the frontier electron density [24] as a reactivity index. He pointed out that during the course of a reaction the HOMO–LUMO interactions become more dominant over the other terms. He further stated that the increase in the electron density in the intermolecular region originates from the overlapping of the HOMO and the LUMO between reactant and reagent [25,26] and that the nodal properties of the HOMO and the LUMO are important in predicting what change in molecular shape will take place.

Fukui and Fujimoto formulated the following rule for the frontier-controlled reactions:

"The majority of chemical reactions are liable to take place at the position and in the direction where the overlapping of the HOMO and the LUMO of respective reactants is at its maximum; in an electron

donating species, HOMO predominates in the overlapping interaction, while the LUMO does so in an electron accepting reactant; in the reacting species which possess singly occupied molecular orbitals these play part of HOMO or LUMO or of both."

This can be compared with the rule formulated by Parr and Yang for Eq. (6), of two different sites with generally similar dispositions for reacting with a given reagent, the reagent prefers the one which on the reagent's approach is associated with the maximum response of the systems electronic chemical potential Eq. (3).

2.2. How to obtain the chemical structure of a molecular system

The electronic structure and the electronic properties are best obtained directly from the Schrödinger equation of the molecular system. The usual approximations have to be applied however, the Born Oppenheimer approximation [27,28] states that, due to the huge difference in mass between the nuclei and the electrons, we can separate the wave function of a system in two factors, a nuclear and an electronic wave function.

This implies that the nuclear positions are treated parametrically into the electronic part and that we have to solve an electronic Schrödinger equation. This approximation enables us to treat molecular systems. An important consequence of this is that we must carefully select meaningful nuclear co-ordinates to obtain meaningful properties. The non-linear electronic Schrödinger equation can then be solved by means of the Hartree–Fock approximation [29], which implies the use of the variational theorem with Slater determinants as trial functions. The mathematical details of this approximation can be skipped, but it has a number of important consequences:

- every electron in the system is described by a one electron wave function,
- each electron moves in the field of the nuclei and the average field of all other electrons,
- it takes the repulsive force between electrons of equal spin into account (exchange repulsion) or the Pauli's exclusion principle,
- the Coulomb repulsion between two electrons of opposite spin occupying the same energy level is not accounted for and results into a correlation energy correction.

The molecular one electron orbitals can be expressed as linear combinations of hydrogen like atomic orbitals centred on the atoms that constitute the molecule and the expansion coefficients are used as variational parameters. In the Roothaan–Hall–Hartree–Fock [30] equations (RHF) two electrons of opposite spin occupying the same energy level have the same spatial part while the Pople–Nesbeth–Hartree–Fock [31] equations (UHF) give electrons of opposite spin different spatial functions. The former are generally used for closed shell systems the latter for open shell system (e.g. radicals). These equations produce an approximate wave function and energy of the system and the various quantities given in Eqs. (3)–(6) can be obtained from them.

This is the famous linear combination of atomic orbitals approach. The Hartree–Fock equations are extensively documented in the literature and can be obtained from all commercial ab initio software packages. The calculation were performed with Gaussian 98 W [32].Conceptual methods have been developed that facilitate the interpretation of the wave function and related properties. Mulliken [33] developed a number of closely related charge distributions based on the LCAO-MO wave function. In his original publication he explained the concepts very well. Weinhold and co-workers [34,35] developed a more sophisticated method to analyse LCAO-MO wave functions, the natural bond orbital (NBO) analysis method. With this method we can directly obtain the electronic structure of a molecular system in terms of overlapping and interacting atom-centred-hybrid-orbitals. The NBO method consists of applying a set of mathematical procedures to the density matrix (that is obtained automatically from the Roothaan–Hall and the Pople–Nesbet equations) to obtain the natural atomic orbitals (NAO's). The NAO's can be used to calculate a population analysis [36]. The density matrix expressed in terms of the NAO can then be partitioned according to the occupation of the NAO's. NAO's of high occupancy (>1.999 e) are core orbitals and eigenvectors of one-centre blocks of high occupancy (>1.9 e) are of lone pair type. Two centre blocks are used to obtain bond eigenvectors. It is also possible to identify low occupancy antibonding and

Rydberg orbitals. A localisation procedure is then applied by minimising the coupling between the highly occupied non-core elements and the low occupied elements. With NBO analysis methods we obtain a complete quantitative picture of the Lewis structure including information about hybridisation effects and bond polarisation in term of natural localised molecular orbitals. Interactions between highly occupied structures and low occupied structures can be used to study non-covalence effects, (e.g. van der Waals complexes).

For the UHF case one obtains different hybrids for different spins [37,38] so we can apply the method to radicals too.

Yang and Mortier [39] proposed the use of the condensed Fukui function

$$f_k^+ = q_k(N+1) - q_k(N) \tag{11}$$

$$f_k^- = q_k(N) - q_k(N-1) \tag{12}$$

$$f_k^0 = \tfrac{1}{2}[q_k(N+1) - q_k(N-1)] \tag{13}$$

with q the Mulliken charge of atom k in the ground state system with N electrons and the system with $N+1$ and $N-1$ electrons calculated with the same nuclear conformation as the system with N electrons.

In the SCF-MO theory localised molecular orbitals are an equivalent representation of the physical system as the canonical molecular orbitals from which they are obtained. NAO's and NLMO's have an associated electronic occupation and they can thus uniquely partition the electron density. This one to one mapping allows us to attribute a chemically relevant meaning to each partition. Because differentiation and integration are commutative operators it is possible to incorporate the NAO and NLMO occupations in Eq. (6) to obtain a natural condensed Fukui function (NCFF). Here we must make use of the different orbitals for different spins approach. An equivalent explanation can be given, when we calculate how the electronic system changes when it comes into contact with a hypothetical atom of $+\infty$ electronegativity we obtain f^- or f^+ if the hypothetical atom has $-\infty$ electronegativity. (For a short tutorial about NBO analysis see [53].)

3. Results and discussion

3.1. The basic model: development and initial assessment

Loverix et al. [7] showed that RNAse T1 is capable of catalysing the cycling between 3′GMP and c2′, 3′GMP. Therefore, it seemed logical to use the X-ray data from the RNAse T1/3′GMP [40] complex. Kinetic experiments showed that the residues His40, His92, Glu58, Tyr38, Phe100 are involved in the catalytic reaction while Arg77 is thought to be involved due to its charge and proximity to the active site. Therefore, I consider these residues collectively as a functional group of the enzyme. In chemistry local properties of functional groups are transferable, therefore it is useful to calculate these local properties in isolation. Moreover it has been shown that NBO's are inherently more transferable [41] than localised molecular orbitals often by a factor 2–4.

I completed the model by adding hydrogens (X-ray diffraction cannot "see" hydrogens). Hydrogens that were not part of ionizable groups or that did not have any conformational freedom were assigned standard bond lengths and angles.

Experimental research revealed that His40, His92 and Arg77 must be protonated and Glu58 is unprotonated. There is no information about the protonation of the substrate phosphate group.

As a consequence I constructed a model that incorporated all amino acids formerly mentioned (H40, H92, E58, Y38, F100, R77) the 3′GMP substrate and water 818 (PDB file ID). The hydrogens connected to the $N\delta$ and the $N\varepsilon$ of both histidine residues, all hydrogens of the aromatic phenylalanine ring, the hydroxyl hydrogen of tyrosine and all hydrogens attached to the nitrogens of the arginine group, the 2′ hydroxyl hydrogen of 3′GMP and the hydrogens of the water molecule were assigned guessed positions. I allowed these hydrogens to relax in the presence of the unprotonated phosphate group at the PM3 [2] [42,43] level (of computational accuracy) which resulted in the abstraction of a proton from the His92. I concluded that this structure has no chemical meaning

[2] PM3 is a semiempirical method that has been used for technical reasons here, it is available with many commercial software packages.

since experimental evidence demonstrated that His92 must be protonated. I then performed three relaxation calculations at the PM3 level. In each calculation, I now added a proton to one of the three stereochemically different phosphate oxygen's (the fourth oxygen constitutes the phosphoester linkage). This revealed the position of the proton on the phosphate group. It is located on the phosphate oxygen closest to the Glu58, forming a hydrogen bridge with Glu58. In that model the two other phosphate oxygen's formed a hydrogen bridge with His92 and Tyr38. All geometries obtained at the PM3 level were recalculated at the RHF/3-21G [44] [3] and the B3LYP/3-21G [45,46] [4] level. These calculations confirmed the results from PM3. The same hydrogen's plus the 5′ hydroxyl hydrogen of the substrate molecule were allowed to relax at the RHF/3-21G level in order to get a more accurate geometry (model 1). [5]

The structural data from the X-ray diffraction study (revealing the positions of the heavy atoms C, N, O, P) are now supplemented with the positions of the H atoms obtained from ab initio calculations. This structure demonstrates how Glu58 prefers to form a strong hydrogen bridge with the singly protonated phophate group of the 3′GMP rather than with the 2′OH of the ribose ring of 3′GMP. It is generally accepted from experimental evidence that the 2′OH must be activated, otherwise their is no catalytic activity. This demonstrates how 3′GMP prevents Glu58 from activating the 2′OH group and thus demonstrates the inhibitory mechanism of 3′GMP. A dinucleotide cannot do this since there is simply no proton available for H-bonding. It also illustrates how protons can play a key role in the regulation of biological processes and it is an example of product inhibition.

Because of this, the reactivity indexes calculated with the model geometry now available will probably not give information about a possible nucleophilic attack of the 2′OH group on the phosphate. Loverix et al. [7] reported the cycling between 3′GMP and c2′, 3′GMP. A detailed investigation of the interaction between the active site and the phosphate group must be performed in order to reveal this apparent contradiction.

3.2. The basic model: refinement

The guanine ring and the 5′ CH_2OH group of 3′GMP are not directly involved in the reaction. I replaced the guanine ring and the 5′ CH_2OH group with hydrogen's and performed a NBO analysis of this system and then compared these results with the results from an NBO analysis performed on 3′GMP. This showed that the electronic structure of the phosphate and the 2′, 3′ portion of the ribose ring were practically identical in both systems. I performed these calculations with different basis sets, this showed that the d-orbitals are a lot more important on the phosphate atom than on the other atoms. The lone pairs on the oxygen's interact with these orbitals, therefore we can conclude that they are part of a delocalised structure. Calculations at the MP2 level revealed that with a correlated wave function the lone pairs on the phosphate oxygen's tend to interact more with the phosphate atom than in the uncorrelated wave function. The properties were not sufficiently altered as to justify the rejection of an uncorrelated wave function for modelling purposes. The phosphate group cannot be modelled without the use of d-orbitals though.

A similar analysis was done with the amino acids, which revealed that the amino acid part had little influence on the electronic structure of the side chains, no d-orbitals were of any particular importance. Based on these calculations I constructed a second model which contains only the essential part of the functional group it will be used in the sequel.

3.3. Calculations and results

The properties of the individual amino acid side chains (in their protonated and deprotonated forms) were calculated, with the geometry obtained from an optimisation of these at the RHF/6-31G(d) level (i.e. not with the geometry obtained from the crystal structure). They will serve as a reference system and as an illustration of the use of the NCFF. I also performed a calculation of all amino acid residues, as a supermolecular complex, in the absence of substrate. In this structure the amino acid residues maintained

[3] The term behind the slash stands for the atomic basis functions being used, for an explanation please see [44].

[4] This indicates that the Kohn Sham equations (which can include correlation effects) have been used rather that the Hartree–Fock equation.

[5] Exact nuclear co-ordinates of this model can be obtained upon request from the author.

their electronic properties and there were no important charge transfer interactions between them only multipole interactions. This result is not unexpected. The interactions of the individual amino acid residues with the substrate (i.e. substrate + one amino acid) were also investigated and compared with the results obtained from a model containing all relevant parts together. This provided very interesting information.

3.4. Results and conclusions for the amino acid residues

Term (9) contains the most important local properties of the system, the Coulomb interaction and the HOMO–LUMO interaction. The natural charge distribution will serve as a Coulomb interaction index. The natural condensed Fukui function (which is very useful) and the condensed Fukui function will be used to investigate the frontier orbitals. The results of a full NBO analysis (calculated with the closed shell system) contain valuable information about the intramolecular interactions. The fragments and the atoms in the fragments will be named as applicable in PDB files.

3.5. Results for Glu58 (Figure 1a)

The interpretation of the reactivity indexes refers to the protonation of the carboxyl group. The interpretation of the charges is trivial. The NBO analyses of the ion shows three lone pairs on both oxygen's (one sp and two p-type) and one lone pair on the carboxyl carbon. On each oxygen one p-type lone pair interacts heavily with the lone pair on the carbon and with the antibond on the opposing C–O bond, this is typical for delocalization stabilisation [47–49] (see arrows identified by no. 1, Fig. 1a). If I looked at the left derivative of the NCFF ($=f^-$) it showed that both oxygen's and the carboxyl carbon lose one p-type orbital, and only one double bond is formed between the carboxyl carbon and an oxygen (see arrows identified by no. 2, Fig. 1a). Later I investigated the structure after protonation and there the bond between the single bonded oxygen and the proton contains a hybrid of sp type on the oxygen. The NCFF thus correctly predicts the covalent changes that will happen during a Lewis acid/base interaction. The right derivative of the Fukui function of this molecule has no much meaning, because a counterpoise calculation proved that the result is a basis set artefact. An empty basis function 5 Å from the molecule was the Fukui function.

3.6. Phe100 (Figure 1b)

The charges and the NBO analysis are in complete agreement with what can be expected for such a molecule. The interpretation of the Fukui function (here f^-) is tricky. The NCFF locates a low occupied p-type lone pair on the Cg and the Cz (see block arrows Fig. 1b).

There is a strong interaction with the hybrid on the Cd1 and the Ce2, respectively, (see arrows Fig. 1b). This explains the *ortho*/*para* orientation of an electrophilic aromatic substitution at toluene. If the electrophile attacks the Cz, the para product will be formed. An attack on the Cg cannot force the methyl group to leave but, due to the delocalization interaction with the Cd1 the *ortho* product will be formed. There is no reason for a meta product.

3.7. His92 and His40 (Figure 1c)

The electronic structure of the imidazolium ion obtained from NBO analysis shows that the nitrogens are most negatively charged, and the Ce1 carbon is most positively charged. All covalent bonds formed with the nitrogens are strongly polarised towards the nitrogen. This indicates that ionic forces are also important in this molecule. The right derivative of the Fukui function ($=f^+$)of imidazolium predicts a possible nucleophilic attack on the Ce1. The NCFF locates a low occupied lone pair on the Ce1 (block arrow with no. 1, Fig. 1c) that is strongly interacting with the lone pairs of the nitrogens (justifying the relatively high values there for the Fukui function) (see arrows with no. 2, Fig. 1c). The analysis of unprotonated imidazole showed that this system has a very similar electronic structure as the imidazolium ion. Surprisingly the f^- predicts no electrophilic attack on the nitrogens, but on the Cg, Cd2 and to a lesser extent on the Ce1 (see block arrows with no. 3, Fig. 1c). We still see a protonation of the nitrogens with the formation of a covalent bond. Since this bond is very polarised, Coulomb forces will stabilise it. If I make a detailed comparison between the electronic structures of the protonated and the unprotonated forms, I see that only the polarisation of the Ce1–N bond is different in both

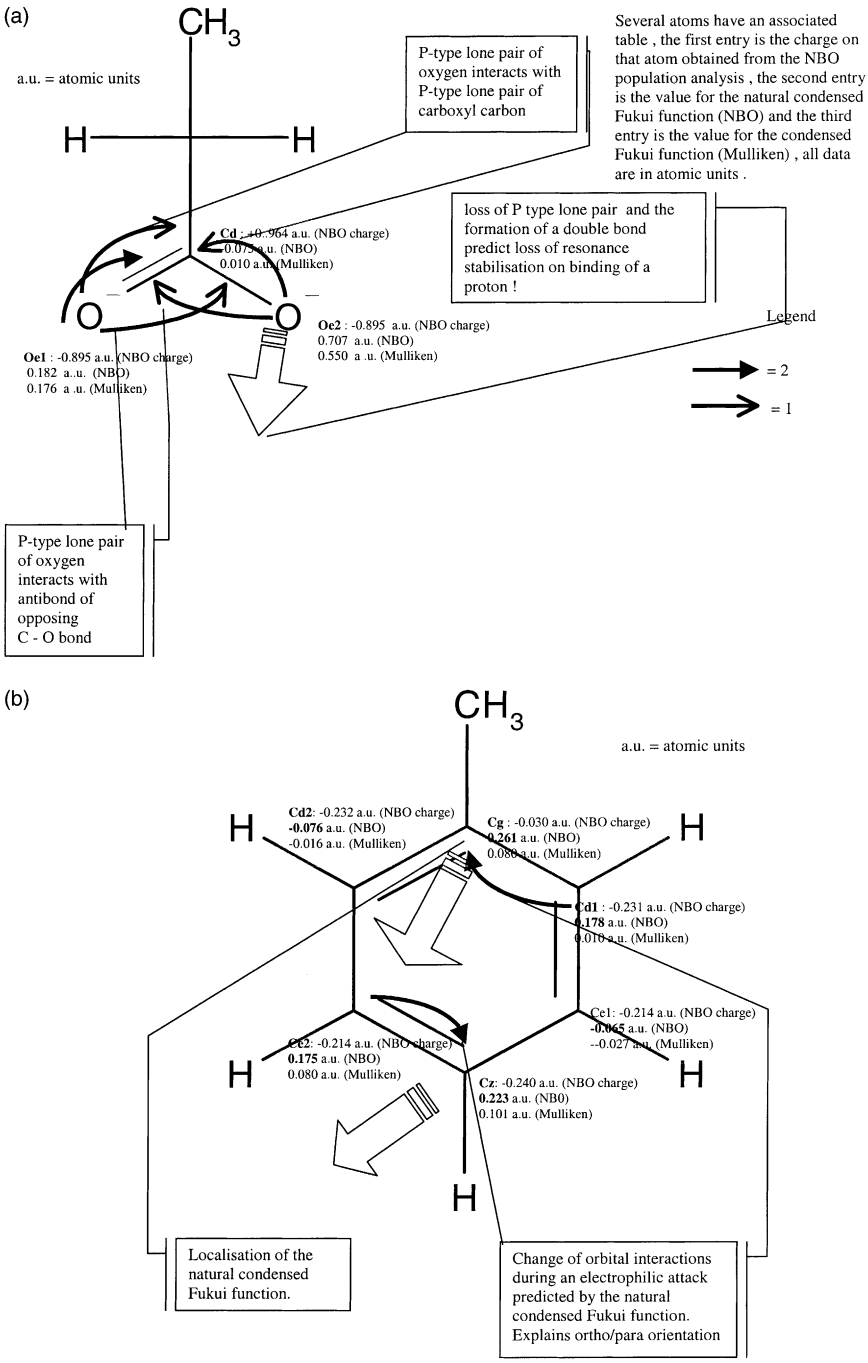

Fig. 1. Isolated amino acids.

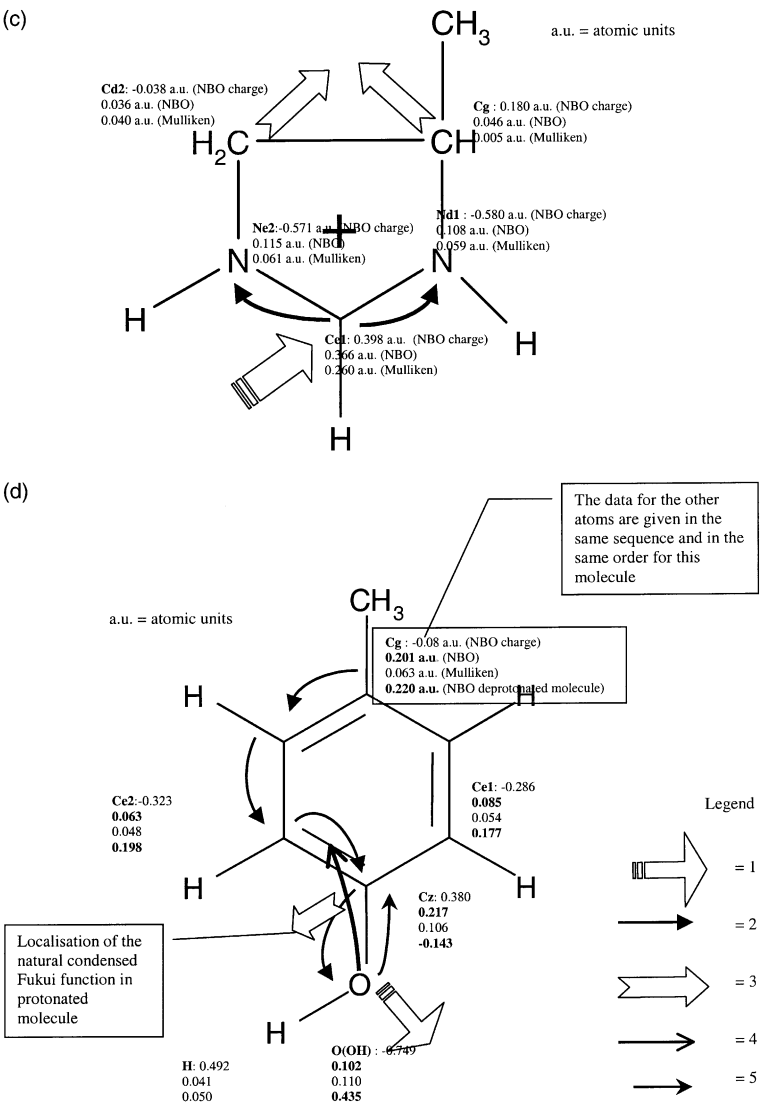

Fig. 1. (*Continued*).

structures. The lone pair at the formerly unprotonated nitrogen retains its local properties after protonation at this site. This proves that the nitrogens are hard centres and a protonation reaction at the nitrogen is not frontier-controlled.

3.8. Tyr38 (Figure 1d)

The NBO structure of this molecule agrees with general knowledge, but the lone pair on the hydroxyl oxygen interacts with the aromatic ring (see arrow with no. 4, Fig. 1d) and is thus also involved in resonance stabilisation. The interpretation of f^- is analogous to the Phe100 case. Here the lone pair of the hydroxyl oxygen interacts with the low occupied lone pair on Cz (see arrow with no. 5, Fig. 1d). The f^- for the molecule with the hydroxyl group deprotonated was also calculated. A beta lone pair on the O(OH) oxygen disappeared, causing an electron transfer from the Cg via the Cd2 to the Ce2 and the Cz (see arrows with

no. 2, Fig. 1d). A double bond was formed between the oxygen and the Cz in the beta system (=the beta electrons) that is responsible for the negative value at Cz. The alpha system reacted with an opposite electron transfer, but only partially compensated at the Cg.

3.9. Arg77

The interaction of arginine with the other parts of the functional group has only an electrostatic component. Several properties, which I obtained were interesting on their own right, but had no relation with the problem at hand and therefore, I will not treat them.

3.10. Substrate molecule (Figure 2, [52])

The phosphate group in the substrate molecule is important. The P–3′OR and the P–OH single bonds are very polarised, as a consequence they are almost ionic. The Mulliken bonding index shows no much bonding density between them. All lone pairs of the four oxygen's have a strong interaction with the spd system on the phosphorus atom (see arrows). This indicates delocalization and partial bond formation, and adds a non-ionic character to the bond. The f^- indicates that a lone pair on the oxygen can be involved in an interaction with a Lewis acid (block arrows). When I put d-orbitals on the phosphate group alone, the system was practically not different from the system with d-orbitals on all atoms (Fig. 2).

3.11. Interactions of the individual side chains with the substrate

NBO analysis can be used to investigate non-multipole intermolecular interactions. In NBO analysis hydrogen bonds are characterised by a delocalisation of the lone pair of the electron donor into the antibond associated with the interacting H–X bond [50,51]. I performed an NBO analysis on a supermolecule of the substrate and one specific amino acid residue in the absence of all other atoms. The results obtained from these calculations will be used to facilitate the interpretation of the data obtained from the calculations on the complete functional group in interaction with the substrate.

3.12. His40–substrate interaction

Here I found a typical hydrogen bond between a lone pair on the 2′O and the Ne2–H antibond on the histidine residue. Delocalisation of an lone pair in an H–X antibond is typical for all hydrogen bridges [35]. There are no additional important orbital interactions between this residue and the substrate.

3.13. His92–substrate interaction

The orbital interactions between His92 and the phosphate group are different from those observed between His40 and the 2′O group on the substrate. The lone pair antibond interaction is much stronger; there is an unusual Rydberg population on the hydrogen attached to the Ne2 and the Cd2–Ne2 antibond is also participating in the interaction. Taken together, this shows that the negative charge on the phosphate group is delocalising in the imidazolium ion system with resonance stabilisation as a consequence. So we have a hydrogen bond with resonance stabilisation.

3.14. Tyr38–substrate interaction

Two lone pairs located on the same oxygen of the phosphate group interact with the antibond of the hydroxyl group; there is a Rydberg population on the hydroxyl hydrogen and an intermolecular antibond/antibond interaction between the P–O antibond and tyrosine hydroxyl antibond. Taken together these indicate very strong delocalization stabilisation and an extra stabilisation due to resonance between the tyrosine residue and phosphate group.

3.15. Arg77–substrate interaction

There are no important orbital interactions between Arg77 and the substrate. Therefore, I conclude that the role of Arg77 in the active site of the enzyme will be electrostatic of nature.

3.16. Phe100–substrate interaction

The structure of the phosphate group, which was already strongly delocalised due to the interaction between the lone pairs on the oxygen's and the spd system on the phosphate group, becomes even more

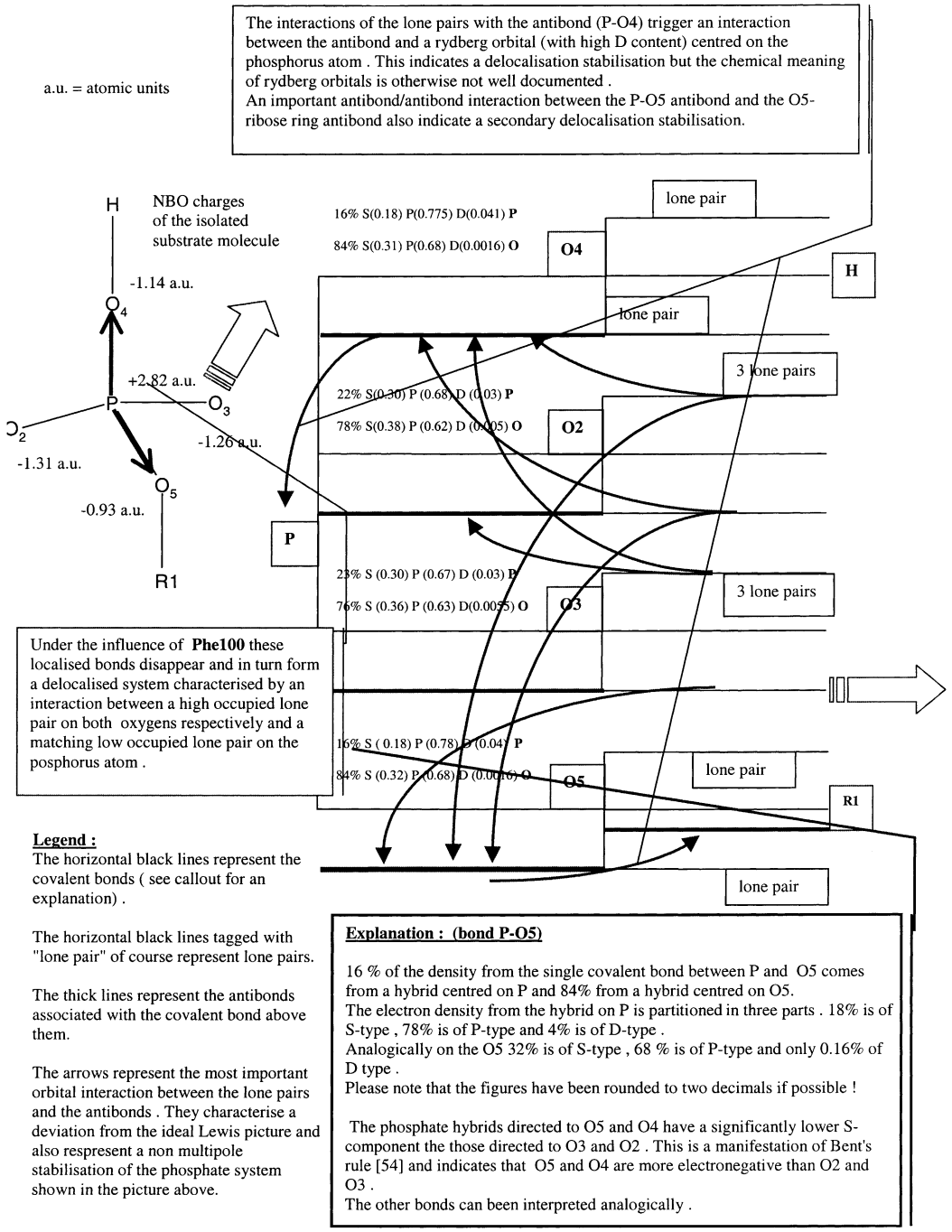

Fig. 2. Phosphate group of the isolated substrate molecule.

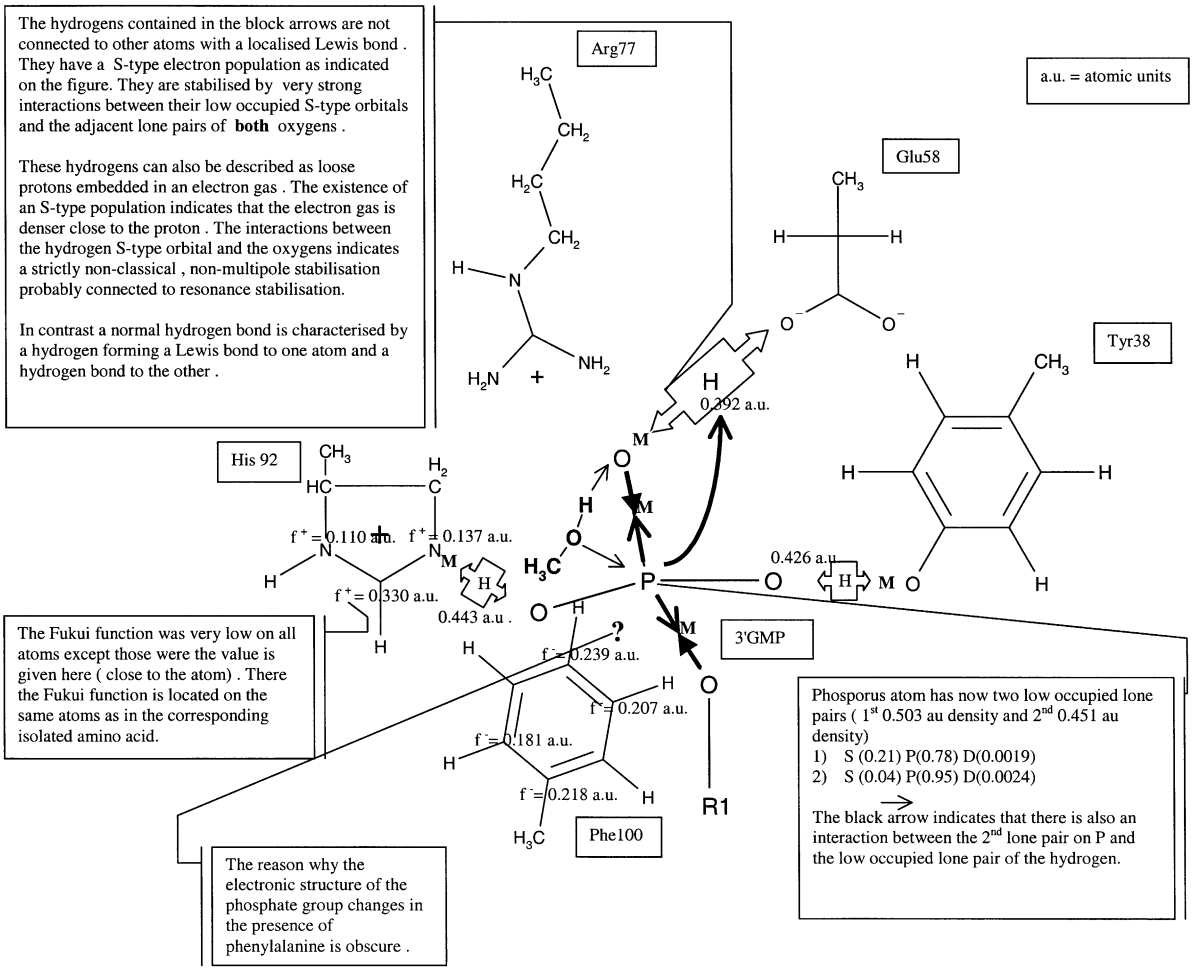

Fig. 3. Active site interactions.

delocalised in this model. The structure of the phosphate group is not well described by considering only a localised single bond at P–3′OR and at P–OH. A structure now containing four lone pairs on these oxygen's and two low occupied lone pairs on the phosphorus atom now becomes as important as the structure described previously (see arrows on phosphate group, Fig. 2 and the callout). In the isolated substrate molecule (as shown in Fig. 2) this resonance structure has 2.189% non-lewis density and was therefore not considered because the most localised system had 1.257% non-lewis density and had precedence over the former (see natural resonance theory) [47,48].

In the model considered here no difference in non-Lewis occupancy between the two resonance structures considered was found any more.

3.17. Crystal water–substrate interaction

The crystal water 818 only has a relatively weak charge transfer interaction with the phosphate oxygen lone pair indicating a classical hydrogen bond.

3.18. Properties of the major functional group

The functional group of interest can now be limited to those residues that directly interact with the

phosphate group of the substrate; a 6-31G(d) basis was used for the phosphate group and a 6-31G basis for the other atoms in the system (see Fig. 3).

The NBO analysis of the interaction between the substrate and the active site residues Glu58, His92, Arg77, Phe100 and Tyr38 revealed strong delocalization of the Lewis bonds in the vicinity of the phosphate group. The Lewis structure of the phosphate group was similar to the structure described in the Phe100-substrate model. The Tyr38 hydroxyl hydrogen, the His92 Ne2 hydrogen and the hydrogen attached the phosphate group now lose their Lewis bonds with the parent residues and become embedded in a delocalised system. Surprisingly no lone pair H–X antibond interactions, so typical for hydrogen bonds, were observed any more (see block arrows containing H, Fig. 3).

I performed a Mulliken population analysis to get more information about what was going on here. The overlap population between O(OH)–H of Tyr38, Ne2–H of His92, PO–H, P–OH and P-3′OR for the model considered here was compared with the overlap population in the isolated structures. The results are given in Table 1 (see the bonds tagged with M, Fig. 3).

The electron population on the phosphorus atom decreased with 0.225 e (due to a population change in the 4p atomic orbitals) and the oxygen gained electron density (0.30 e). The f^+ and the f^- were also calculated for this system. The f^+ was located on the His92 and had exactly the same properties as the corresponding Fukui function on the isolated structure of His92, the f^- was completely located on the Phe100 and also had the same properties as on the corresponding reference structure. The values of the Fukui function are given in Fig. 3.

Table 1
Mulliken overlap charges (a.u. = atomic units)[a]

	Functional group/2 (a.u.)	Reference structure/2 (a.u.)
Tyr38 O(OH)–H	0.23	0.26
His92 Ne2–H	0.12	0.29
PO–H	0.12	0.24
P–OH	0.38	0.27
P-3′OR	0.27	0.18

[a] This table shows how the indicated overlap population changes in the functional group with respect to the reference structure.

Since the Glu58 has adopted a conformation typical of inhibitor binding I investigated the properties of the former system in its absence. In the NBO analysis only the PO–H overlap population raised to 0.24 e (its normal value) but the f^- became localised on the Tyr38 where it had distinctly different properties than the f^- on the reference system. The properties were very similar to the reference system with the hydroxyl group deprotonated, only the negative term on the Cz was not present. This is probably because the lone pair on the oxygen formerly involved in double bond formation has found a more suitable partner than the partially filled lone pair on the Cz. The NBO analysis was also performed on this model with a 3-21G-basis set to check for possible basis set artifacts, but the result with this basis set was similar.

4. Conclusions

Of general importance to conceptual chemistry (and biochemistry) is that NBO's are very suitable to interpret the Fukui function. The information we obtain from the NCFF can directly be interpreted with the help of the Fukui rule. Sometimes it is possible to predict the intramolecular covalent changes that will happen during a Lewis acid/base interaction (e.g. Glu58 case) but this has to be done with caution. The equations from the DFT then shows what role the Fukui function plays in the energy change during an Lewis acid/base interaction and so adds to our understanding.

For the enzymatic reaction mechanism it can be concluded that the phosphate group is not going to experience a frontier-controlled nucleophilic attack without a significant change in its structure. The f^+ does not indicate any sensitivity not in the functional group and not in the isolated substrate molecule. The f^+ and the f^- are located on the His92 and the Phe100, respectively. This may be connected to the functional interaction that was measured by Doumen et al. [6] between His92 and Phe100 during the binding of a dinucleotide substrate, but may also be caused by the inhibitory conformation adopted by Glu58.

This does not yet explain the cycling hypothesis of Loverix et al. [7]. They incubated 3′GMP with 40%

methanol and RNAse T1 to obtain c2′, 3′GMP and GpMe. (The experiments they performed with RNAse A are of no use here since RNAse A does not have a functional analog of Glu58).

The NBO analysis reveals significant changes in the electronic structure of the phosphate group and its surroundings. In at least one important resonance structure the phosphate group resembles the electronic structure of an $RPO_2^{2-}H$ intermediate (see Fig. 3) which has two occupied lone pairs (the resonance structure in Fig. 3 has low occupied lone pairs). The hydrogen's surrounding the phosphate group have undergone dramatic changes in their electronic structure indicating an unusual strong interaction. I think this means that the active site residues Tyr38 and His92 are in a process of pulling the oxygen's away of the phosphorus atom. This would allow the lone pairs of the methanol oxygen to interact with the low occupied lone pairs on the phosphor atom (as indicated in Fig. 3). This in turn would allow replacement of the OH group with a CH_3O group. Glu58 will then lose its hydrogen bond with the phosphate group and will probably adopt a conformation typical for a catalytic site, where it interacts with the 2′OH of 3′GMP. The enzyme can then catalyse the formation of c2′, 3′GMP from 3′GpMe in the usual way.

The results of the NBO analysis do more than just assisting in the explanation of an observed reaction. The hydrogen's participate in a delocalised system covering many atoms rather than forming hydrogen bonds. Therefore the hydrogen's initiate the formation of an electronic structure that is completely different from the structure of the substrate that can exist outside the active site of the enzyme. The results of the calculations with Glu58 left out demonstrate this too. Phe100 alone causes the same shift in the weight of the resonance structure concerning the P-3′OR and the P–OH bonds as the entire functional group. This is indicative for a possible role of Phe100 in the catalytic mechanism as Doumen et al. [6] said.

Finally, the intense change in orbital interactions observed in the vicinity of the chemical group that is the subject of the catalytic mechanism, stands in sharp contrast with the almost complete absence of orbital interactions between the active site residues without bound substrate. So what is described here may be typical for enzyme catalysis.

Acknowledgements

I wish to thank my brother Tom for the IT support I obtained from him, during this project. I also want to thank Prof. F. Weinhold for sending me the WISC-TCI-689 report.

References

[1] K. Sato, F. Egami, J. Biochem. Tokyo 44 (1957) 753–767.
[2] F. Eckstein, H.H. Schultz, H. Ruterjans, W. Haar, W. Maurer, Biochemistry 11 (1972) 3507–3512.
[3] H.L. Osterman, F.G Waltz Jr., Biochemistry 17 (1978) 4124–4130.
[4] J. Steyaert, K. Hallenga, L. Wyns, P. Stanssens, Biochemistry 29 (1990) 9064–9072.
[5] J. Steyaert, A. Fattah Haikal, L. Wijns, P. Stanssens, Biochemistry 30 (1991) 8666–8670.
[6] J. Doumen, M. Gonciarz, I. Zegers, R. Loris, L. Wyns, J. Steyaert, Protein Sci. 5 (1996) 1523–1530.
[7] S. Loverix, G. Laus, J.C. Martins, L. Wyns, J. Steyaert, Eur. J. Biochem. 257 (1998) 286–290.
[8] R.G. Pearson, J. Am. Chem. Soc. 85 (1963) 3533–3539.
[9] P.K. Chattaraj, H. Lee, R. Parr, HSAB principle, J. Am. Chem. Soc. 113 (1991) 1855–1856.
[10] R.T. Sanderson, Science 114 (1951) 670–672.
[11] R.G. Parr, P.K. Chattaraj, J. Am. Chem. Soc. 113 (1991) 1854–1855.
[12] R.G. Parr, W. Yang, Density Functional Theory of Atoms and Molecules, Oxford University Press, New York, 1989, pp. 70–86.
[13] R.G. Parr, W. Yang, Density Functional Theory of Atoms and Molecules, Oxford University Press, New York, 1989, pp. 74–75 and pp. 90–95.
[14] R.G. Parr, W. Yang, Density Functional Theory of Atoms and Molecules, Oxford University Press, New York, 1989, pp. 87–88
[15] P. Hohenberg, W. Kohn, Phys. Rev. 136 (1964) B864–B871.
[16] R.G. Parr, W. Yang, Density Functional Theory of Atoms and Molecules, Oxford University Press, New York, 1989, pp. 99–101.
[17] M. Berkowitz, R.G. Parr, J. Chem. Phys. 88 (1988) 2554–2557.
[18] Y. Li, J.N.S. Evans, J. Am. Chem. Soc. 117 (1995) 7756–7759.
[19] R.G. Parr, W. Yang, Density Functional Theory of Atoms and Molecules, Oxford University Press, New York, 1989, p. 15 and 227.
[20] R.G. Parr, R.G. Pearson, J. Am. Chem. Soc. 105 (1983) 7512.
[21] R.G. Parr, W. Yang, Density Functional Theory of Atoms and Molecules, Oxford University Press, New York, 1989, pp. 226–227
[22] G. Klopman, Chemical Reactivity and Reaction Path's, Wiley, New York, 1974, pp. 59–67.

[23] G. Klopman, Chemical Reactivity and Reaction Path's, Wiley, New York, 1974, pp. 23–54.
[24] K. Fukui, T. Yonezawa, H. Shingu, J. Chem. Phys. 20 (1952) 722.
[25] H. Fujimoto, S. Yamabe, K. Fukui, Tetrahedron Lett. 5 (1971) 443.
[26] H. Fujimoto, S. Yamabe, K. Fukui, Bull. Chem. Soc. Jpn. 44 (1971) 2936.
[27] M. Born, J.R. Oppenheimer, Ann. Physik 84 (1927) 457.
[28] B.T. Sutcliffe, Fundamentals of computational quantum chemistry, in: G.H.F. Diercksen, B.T. Sutcliffe, A. Veillard (Eds.), Computational Techniques in Quantum Chemistry, Reidel, Boston, 1975, p. 1.
[29] A. Szabo, N.S. Ostlund, Modern Quantum Chemistry Introduction to Advanced Electronic Structure Theory, Dover, New York, 1996.
[30] C.C.J. Roothaan, Rev. Mod. Phys. 23 (1951) 69.
[31] J.A. Pople, R.K. Nesbet, J. Comput. Phys. 22 (1954) 571.
[32] M.J. Frisch, G.W. Trucks, H.B. Schlegel, G.E. Scuseria, M.A. Robb, J.R. Cheeseman, V.G. Zakrzewski, J.A. Montgomery Jr., R.E. Stratmann, J.C. Burant, S. Dapprich, J.M. Millam, A.D. Daniels, K.N. Kudin, M.C. Strain, O. Farkas, J. Tomasi, V. Barone, M. Cossi, R. Cammi, B. Mennucci, C. Pomelli, C. Adamo, S. Clifford, J. Ochterski, G.A. Petersson, P.Y. Ayala, Q. Cui, K. Morokuma, D.K. Malick, A.D. Rabuck, K. Raghavachari, J.B. Foresman, J. Cioslowski, J.V. Ortiz, A.G. Baboul, B.B. Stefanov, G. Liu, A. Liashenko, P. Piskorz, I. Komaromi, R. Gomperts, R.L. Martin, D.J. Fox, T. Keith, M.A. Al-Laham, C.Y. Peng, A. Nanayakkara, C. Gonzalez, M. Challacombe, P.M.W. Gill, B. Johnson, W. Chen, M.W. Wong, J.L. Andres, C. Gonzalez, M. Head-Gordon, E.S. Replogle, J.A. Pople, Gaussian 98, Revision A.7, Gaussian, Inc., Pittsburgh, PA, 1998.
[33] R.S. Mulliken, J. Chem. Phys. 23 (10) (1955) 1833–1840.
[34] J. Foster, F. Weinhold, Natural hybrid orbitals, J. Am. Chem. Soc. 102 (1980) 7211–7218.
[35] A.E. Reed, L. Curtis, F. Weinhold, Chem. Rev. 88 (1988) 899–926.
[36] A.E. Reed, R.B. Weinstock, F. Weinhold, J. Chem. Phys. 83 (1985) 735–746.
[37] J.E. Carpenter, F. Weinhold, Theoretical Chemistry Institute Report WISC-TCI-689, 1985.
[38] J.E. Carpenter, F. Weinhold, J. Mol. Struct. (Theochem.) 169 (1988) 41–62.
[39] W. Yang, W.J. Mortier, J. Am. Chem. Soc. 108 (1986) 5708–5711.
[40] I. Zegers, R. Loris, G. Dehollander, A. Fattah Haikal, A. Poortmans, J. Steyaert, L. Wyns, Natl. Struct. Biol. 5 (1998) 280.
[41] J.E. Carpenter, F. Weinhold, J. Am. Chem. Soc. 110 (1988) 368–372.
[42] J.J.P. Stewart, J. Comput. Chem. 10 (1989) 209.
[43] J.J.P. Stewart, J. Comput. Chem. 10 (1989) 221.
[44] W.J. Hehre, L. Radon, P.V.R. Schleyer, J.A. Pople, Ab Initio Molecular Orbital Theory, Wiley, New York, 1985.
[45] W. Kohn, L.J. Sham, Phys. Rev. 140 (1965) A1133–A1138.
[46] A.D. Becke, J. Chem. Phys. 98 (1993) 5648.
[47] E.D. Glendening, F. Weinhold, J. Comput. Chem. 9 (6) (1998) 593–609.
[48] E.D. Glendening, F. Weinhold, J. Comput. Chem. 9 (6) (1998) 610–627.
[49] E.D. Glendening, J.K. Badenhoop, F. Weinhold, J. Comput. Chem. 9 (6) (1998) 628–646.
[50] L.A. Curtiss, D.J. Pochatko, A.E. Reed, F. Weinhold, J. Chem. Phys. 82 (1985) 2679–2687.
[51] A.E. Reed, F. Weinhold, L.A. Curtiss, D.J. Pochatko, J. Chem. Phys. 84 (1986) 5687–5705.
[52] H.A. Bent, A Chem. Rev. 61 (1961) 275–311.
[53] www.colby.edu/chemistry/webmo/nbotutor.html.